Chinese J. of Chem. Eng., 8 (4) 326—331 (2000)

Neural Network Approach to Predict Melt Temperature in Injection Molding Processes

WANG Baoguo(王保国)*, GAO Furong(高福荣) and YUE Polock(余宝乐)
Department of Chemical Engineering, Hong Kong University of Science and Technology, Clear Water Bay, Kowloon, Hong Kong, China

Abstract Among the processing conditions of injection molding, temperature of the melt entering the mold plays a significant role in determining the quality of molded parts. In our previous research, a neural network was developed to predict the melt temperature in the barrel during the plastication phase. In this paper, a neural network is proposed to predict the melt temperature at the nozzle exit during the injection phase. A typical two-layer neural network with back propagation learning rules is used to model the relationship between input and output in the injection phase. The preliminary results show that the network works well and may be used for on-line optimization and control of injection molding processes.
Keywords injection molding, neural network, melt temperature

1 INTRODUCTION

Injection molding is a widely used plastics processing method, and plays an important role in the plastics industry due to its high production rates, cost effectiveness and ability to produce complex articles with high precision. It is estimated that approximately 32% by weight of all plastic materials are processed with injection molding machines[1,2]. A typical modern reciprocating screw injection molding machine is schematically shown in Fig. 1[1,3]. It consists of three main units: an injection unit, a clamping unit and a hydraulic unit. The injection unit combines plastication and injection into a single unit (barrel) in which a reciprocating screw is used to plasticize the material and then inject the melt into the mold. The function of the clamping unit is to close, hold and open the mold, and the function of the hydraulic unit is to supply the high pressure during operation. The application of computer in injection molding is mainly focused on mold design and simulation of the melt flow in the mold cavity, while our research interests are in the injection unit.

In a reciprocating screw injection unit as shown in Fig. 1, the plastic is fed to the hopper and then melted in the barrel of the injection molding machine. The melt is transferred to the nozzle of the machine by a rotating screw. The accumulation of the melt at the screw tip forces the screw to retract until a given amount of melt is collected for a shot. The screw is then driven forward to inject the melt into the mold. The melt temperature, to a degree, determines whether a qualified molded part can be produced. The temperature is influenced by the processing conditions such as screw rotation speed, back pressure, and externally applied heat (from barrel heaters). In the plastics industry, the control of melt temperature is indirectly achieved *via* setting of these operating conditions.

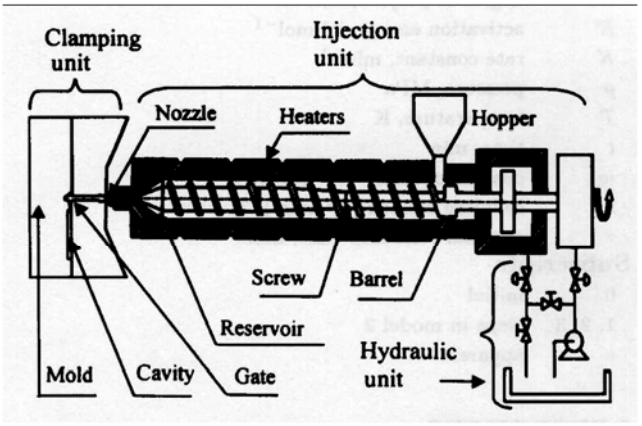

Figure 1 A simplified schematic of a modern reciprocating screw injection molding machine

Melt temperature measured at the cavity gate, as shown in Fig. 1, is an ideal representation of the melt temperature entering the mold cavity. In practice, it is difficult and, in some cases even undesirable, to install a temperature transducer at the cavity gate for each mold. A temperature transducer installed at the nozzle exit can approximately represent the melt temperature into the mold cavity, as there is only a short distance between the nozzle exit and the cavity gate. In this research, the melt temperature measured at

Received 1999-07-20, accepted 1999-12-29.
* To whom correspondence should be addressed. Current address: School of Chemical Engineering, Tianjin University, Tianjin 300072, P. R. China. E-mail: bgwang@public.tpt.tj.cn

the nozzle exit is used to represent the desired melt temperature, which in turn determines the melt viscosity and quality of the molded parts. The exact effect of this temperature is dependent on three factors: (1) the melt temperature distribution in the barrel of the injection molding machine at the plastication phase; (2) the heat conduction between the melt in the barrel and the surrounding at the dwell phase, and (3) the shear heating effect at the injection phase[4]. These three factors are related to the three consecutive phases of the injection molding process: plastication, dwell and injection. The effect of the first two factors (plastication and dwell) on melt temperature was investigated in the previous research using artificial neural networks[4,5]. In the current research, the effect of the injection phase on melt temperature is investigated and some results are presented in this paper. The effect of injection phase on melt temperature is carried out using a commercial software, FIDAP, and the neural network for the on-line prediction of melt temperature is developed on the basis of simulation results.

2 EXPERIMENTAL FACILITY AND PREVIOUS WORK

A ChenHsong JM88MKⅢ (88 ton) reciprocating screw injection molding machine was used in this project with an infra-red melt temperature transducer (Dynisco MTX 935) installed at the nozzle exit. The injection barrel has six barrel heaters (H1 to H6) and one nozzle heater (Hn), and the six barrel heaters are grouped into four heating zones (zone 1 to zone 4) as shown in Fig. 2. The temperature of the nozzle heater is represented by T_n, and the temperature of the four heating zones is represented by T_{z1}, T_{z2}, T_{z3} and T_{z4} respectively. The influence of each individual heating zone on the melt temperature was studied by fractional factorial experimental design[6]. The results showed that the effect of the heating zone 4 on melt temperature is not significant and thus it was not further investigated[4]. Therefore, the operating conditions that affect the melt temperature during the plastication phase are the following seven process parameters: the nozzle heater temperature (T_n), barrel heater temperatures (T_{z1}, T_{z2} and T_{z3}), the screw rotating speed (R_S), back pressure (P_b) and the specified stroke length (S_L).

It is difficult to measure the melt temperature distribution in the barrel. However, if the melt is injected at very low injection velocity, then the shear heating effect due to injection on the melt can be ignored and the melt temperature at the nozzle exit can approximately represent the melt temperature distribution in the barrel reservoir. It is also difficult to establish an accurate mathematical relationship between the plastication conditions and the melt temperature based on the fundamental principles. The input to and the output from the process can, however, be measured. With sufficient input and output data, neural networks can be trained to capture the relationship between the plastication conditions and the melt temperature. With this in mind, air shot experiments at low injection velocity were carried out to measure the melt temperature profile at the nozzle exit.

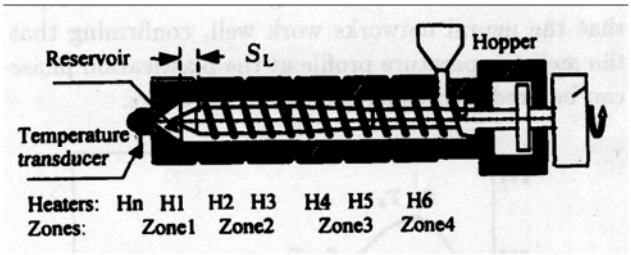

Figure 2 Barrel heaters arrangement

During experiments, the melt temperature (measured at the nozzle exit) and the displacement of the stroke at any given time were recorded, and then the relationship between the melt temperature and the stroke displacement can be established. The temperature profile measured in low injection velocity air shot experiments can be characterized with 7 points as shown in Fig. 3. The horizontal axis represents the stroke displacement and the vertical axis represents the melt temperature measured at the nozzle exit. Points (S_1, T_1) and (S_7, T_7) denote the temperatures when the stroke displacements are zero and 100% of the full stroke length (S_L) respectively. The point (S_3, T_3) represents the maximum temperature and the corresponding stroke displacement. The point (S_2, T_2) denotes the temperature when the stroke displacement equals the average value of S_1 and S_3. Points (S_5, T_5) and (S_6, T_6) represent the temperatures when the stroke displacements are 75% and 90% of the full stroke length respectively. While the point (S_4, T_4) represents the stroke displacement when the temperature is the average value of T_3 and T_5. Therefore, when the six temperatures (T_1, T_2, T_3, T_5, T_6, and T_7) and two stroke displacements (S_3 and S_4) are determined, the 7 points can be obtained and then the temperature profile can be established.

In the previous work[4,5], eight feedforward artificial neural networks (ANNs) have been developed as shown in Fig. 4. Each of the them has two layers: a log-sigmoid hidden layer and a linear output layer. The log-sigmoid neurons (12 to 16) in the hidden layer

of the neural network receives inputs and then transfer their outputs to the output layer of linear neurons which compute the network output. Each network has 7 inputs (T_n, T_{z1}, T_{z2}, T_{z3}, R_S, P_b and S_L) and one of the 8 outputs, T_1, T_2, T_3, T_5, T_6, T_7, S_3 and S_4. The proposed neural networks were trained with 64 sets of experimental data and tested with 10 sets of unused experimental data. The 7 points as shown in Fig. 3 were obtained by use of the 8 outputs from the neural networks and then the temperature profile was fitted by use of cubic spline interpolation. Three sets of experimental data and the corresponding prediction results are shown in Fig. 5. These results show that the neural networks work well, confirming that the melt temperature profile at the plastication phase can be predicted using the neural networks.

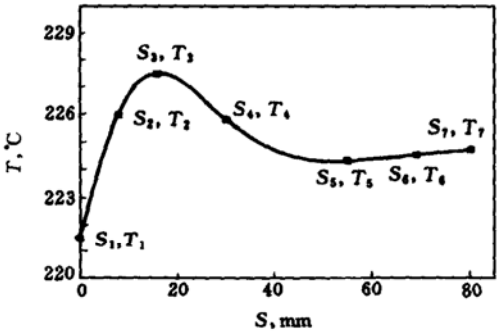

Figure 3 Melt temperature profile representation

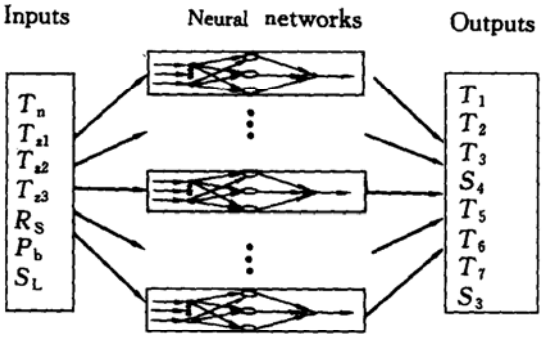

Figure 4 Neural network for the plastication phase

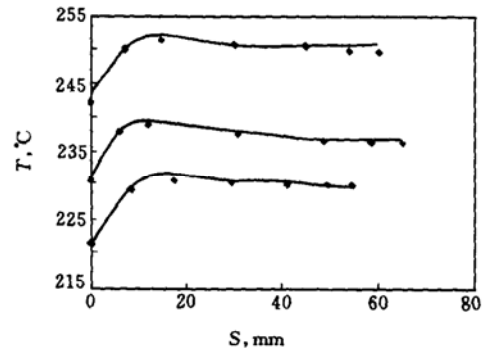

Figure 5 ANN prediction results at the plastication phase

◆ experimental data; ——ANN prediction results

3 FIDAP SIMULATION

With the results from ANNs prediction, the melt temperature during the injection phase can be calculated by use of commercial software FIDAP which is an integrated environment for the simulation of fluid flow problems. The software used in this research is the latest version FIDAP8.0 for PC[7]. It can be executed with or without a graphical user interface and be viewed as an integrated set of components and program modules designed to perform all aspects of the model generation, problem setup, post-processing and solution phases of flow analysis.

The simulation of the injection phase is treated as a fluid mechanics problem coupled with heat transfer, and the screw is considered as a piston with an equivalent cross sectional area. During injection, the screw moves forward and pushes the melt in the barrel into the mold through the nozzle exit. It can be treated as a free boundary problem with a predetermined injection velocity. Although details of the simulation will not be discussed in this paper, the basic inputs and output of the simulation process are shown in Fig. 6.

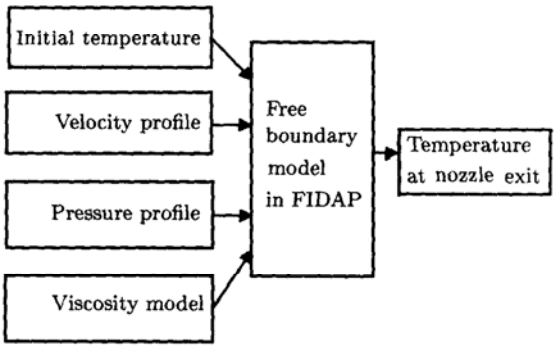

Figure 6 Model structure of FIDAP simulation

The basic inputs to FIDAP are the initial temperature profile, injection velocity as well as pressure. The initial temperature profile is predicted by the ANNs mentioned in Section 2, and the injection velocity is a known operating condition and its corresponding injection pressure profile is taken as the values measured experimentally. The free boundary model is used to simulate the melt flow during injection. The simulation results are processed to obtain the melt temperature profile at the nozzle exit. A typical temperature profile is shown in Fig. 7 and the bulk temperature is taken as the melt temperature during injection.

4 NEURAL NETWORK DEVELOPMENT

As discussed in Section 1, the melt temperature at the nozzle exit plays an important role in determining the product quality and the accurate prediction, and

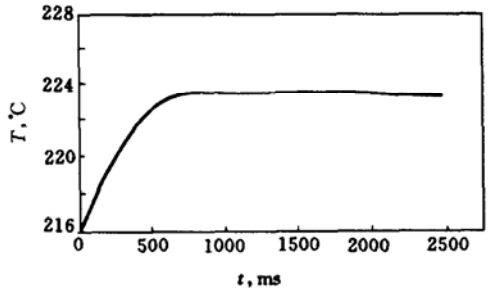

Figure 7 Melt temperature profile at nozzle exit

control of this temperature is a key issue in the plastics industry. Although the melt temperature can be calculated with the help of FIDAP, the calculation process is time-consuming and cannot be used as a model for on-line melt temperature control. Thus, it is necessary to develop an on-line prediction model for real-time optimization and control of injection molding processes. If sufficient input and output data are available by running FIDAP, then a neural network may be built to capture the relationship between input and output and finally it can be used to replace FIDAP for on-line melt temperature prediction and control.

A feed-forward neural network is developed using the typical 2-layer architecture as shown in Fig. 8. The log-sigmoid neurons in the hidden layer of the neural network receive inputs and then send their outputs to the linear output layer which calculates the network output. The 2-layer sigmoid/linear network has been proven to be able to represent any functional relationship between inputs and outputs if the sigmoid layer has enough neurons[8]. The results presented in Section 2 also confirm this point.

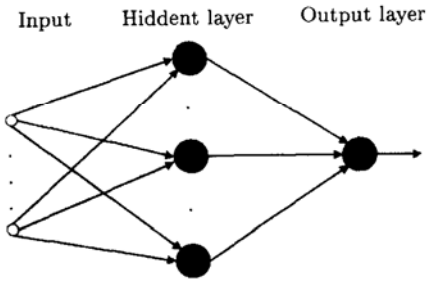

Figure 8 Typical two-layer architecture of neural network

The number of inputs to the network is determined by the problem to be solved. In this circumstance, it is determined by the initial temperature profile, the injection velocity and the corresponding pressure. As discussed in Section 2, the initial temperature profile is determined by the seven operating conditions of the injection molding machine: nozzle heater temperature (T_n), barrel heater temperatures (T_{z1}, T_{z2} and T_{z3}), the screw rotation speed (R_S), back pressure (P_b), the specified stroke length (S_L). Therefore, the inputs to the neural network are: T_n, T_{z1}, T_{z2}, T_{z3}, R_S, P_b, S_L and V (injection velocity). The only one output of the neural network is the bulk melt temperature (T_m).

It is believed that the trained backpropagation networks tend to give reasonable answers when they are deal with unused inputs. This generalization capability makes it possible to train a network on a representative set of input/output pairs and get good results for new inputs without training the network on all possible input/output pairs. The proposed neural network was trained with 70 sets of simulation data and tested with 4 sets of unused data. There are 12 log-sigmoid neurons in the hidden layer and only one linear neuron in the output layer. The ANN training input data are listed in the first eight columns of Table 1, while the ANN training output data are listed in the last column. The 4 sets of testing data and the results are shown in Table 2. T_{exp} represents the bulk melt temperature measured experimentally and T_{ann} represents the bulk melt temperature predicted by the neural network. For the 4 sets of testing data, the maximum prediction error is less than 2 ℃. It shows that the proposed neural network works well and can be used to replace FIDAP for on-line melt temperature prediction in the injection molding process.

5 CONCLUTIONS

In this paper, a neural network is proposed to predict the bulk melt temperature at the nozzle exit during the injection phase. The neural network is trained with simulation results from FIDAP and tested with experimental data. The preliminary results show that the network works well and the bulk melt temperature can be determined in real-time. It seems that such a system has good potential in implementing on-line prediction, optimization and control of melt temperature in injection molding processes.

ACKNOWLEDGEMENTS

The authors would like to thank the financial support of the Croucher Foundation, Hong Kong.

NOMENCLATURE

P_b	back pressure, Pa
R_S	screw rotating speed, min^{-1}
S	stroke displacement, mm
S_L	specified stroke length, mm
T	temperature, ℃
T_m	bulk melt temperature, ℃

Table 1 ANN training data

No.	T_n ℃	T_{z1} ℃	T_{z2} ℃	T_{z3} ℃	R_S min^{-1}	$P_b \times 10^{-5}$ Pa	S_L mm	V $mm \cdot s^{-1}$	T_m ℃
1	200	190	175	155	110	5	80	30	219.8
2	200	190	175	160	100	4.5	70	30	220
3	200	190	175	165	90	4	60	20	221.3
4	200	190	175	165	90	4	60	30	221.7
5	200	190	175	170	80	3.5	50	40	223
6	200	197	187	167	80	4.5	60	20	223.4
7	200	197	187	167	80	4.5	60	40	224.2
8	200	197	187	172	90	5	50	20	225
9	200	197	187	177	100	3.5	80	30	223
10	200	197	187	182	110	4	70	30	223.3
11	200	194	194	174	90	3.5	70	20	221.8
12	200	194	194	179	80	4	80	40	222.7
13	200	194	194	184	110	4.5	50	40	225.8
14	200	194	194	189	100	5	60	20	224.4
15	200	194	194	189	100	5	60	30	224.8
16	200	200	195	175	100	4	50	30	225.8
17	200	200	195	180	110	3.5	60	30	225.6
18	200	200	195	185	80	5	70	40	226.3
19	200	200	195	190	90	4.5	80	20	225.2
20	210	200	195	175	90	3.5	70	20	230
21	210	200	195	180	80	4	80	30	229.6
22	210	200	195	185	110	4.5	50	20	234.3
23	210	200	195	190	100	5	60	40	235.1
24	210	200	195	190	100	5	60	20	234.3
25	210	204	194	174	110	5	80	20	231.6
26	210	204	194	179	100	4.5	70	40	233.3
27	210	204	194	184	90	4	60	30	234.5
28	210	204	194	184	90	4	60	40	235
29	210	204	194	189	80	3.5	50	30	236.5
30	210	207	207	187	100	4	50	40	241.1
31	210	207	207	192	110	3.5	60	20	239.1
32	210	207	207	192	110	3.5	60	30	240.1
33	210	207	207	197	80	5	70	30	23.5
34	210	207	207	202	90	4.5	80	30	239.7
35	210	210	195	175	80	4.5	60	30	234.4
36	210	210	195	180	90	5	50	20	234.3
37	210	210	195	185	100	3.5	80	20	231.9
38	210	210	195	185	100	3.5	80	40	232.8
39	210	210	195	190	110	4	70	20	232.8
40	220	214	199	184	110	3.5	60	40	240.1
41	220	214	199	189	80	5	70	30	240.1
42	220	214	199	194	90	4.5	80	30	233.9
43	220	210	210	190	80	4.5	60	20	246.2
44	220	210	210	195	90	5	50	30	245.7
45	220	210	210	200	100	3.5	80	20	242.2
46	220	210	210	205	110	4	70	40	244.7
47	220	220	210	190	90	3.5	70	30	243.7
48	220	220	210	195	80	4	80	20	243.1
49	220	220	210	200	110	4.5	50	40	246.7
50	220	220	210	205	100	5	60	20	245
51	220	217	212	192	110	5	80	40	243.5
52	220	217	212	197	100	4.5	70	20	243.8
53	220	217	212	202	90	4	60	30	246.5

Table 1 (continued)

No.	T_n ℃	T_{z1} ℃	T_{z2} ℃	T_{z3} ℃	R_S min^{-1}	$P_b \times 10^{-5}$ Pa	S_L mm	V $mm \cdot s^{-1}$	T_m ℃
54	220	217	212	207	80	3.5	50	30	248.1
55	230	220	210	190	100	4	50	20	253
56	230	220	210	195	110	3.5	60	30	252.7
57	230	220	210	200	80	5	70	20	252.4
58	230	220	210	205	90	4.5	80	40	252.2
59	230	227	212	192	90	3.5	70	40	252.5
60	230	227	212	197	80	4	80	20	251.7
61	230	227	212	202	110	4.5	50	30	255.7
62	230	227	212	207	100	5	60	40	255.3
63	230	224	219	199	80	4.5	60	20	253.5
64	230	224	219	204	90	5	50	40	257.1
65	230	224	219	209	100	3.5	80	30	254.6
66	230	224	219	214	110	4	70	30	254.9
67	230	230	230	210	110	5	80	30	258.6
68	230	230	230	215	100	4.5	70	20	259.9
69	230	230	230	220	90	4	60	40	262.7
70	230	230	230	225	80	3.5	50	20	263.4

Table 2 ANN prediction results

No.	T_n ℃	T_{z1} ℃	T_{z2} ℃	T_{z3} ℃	R_S min^{-1}	$P_b \times 10^{-5}$ Pa	S_L mm	V $mm \cdot s^{-1}$	T_{exp} ℃	T_{ann} ℃	Error ℃
1	200	200	195	180	110	3.5	60	20	225.1	224.6	0.5
2	210	200	195	190	100	5	60	30	234.6	234.3	0.3
3	210	207	207	192	110	3.5	60	40	240.8	242.4	−1.6
4	220	210	210	190	80	4.5	60	30	245.2	245.7	−0.5

T_n nozzle heater temperature, ℃

T_{z1} barrel heater temperature of heating zone 1, ℃

T_{z2} barrel heater temperature of heating zone 2, ℃

T_{z3} barrel heater temperature of heating zone 3, ℃

T_{ann} bulk melt temperature predicted by the neural network, ℃

T_{exp} bulk melt temperature measured experimentally, ℃

t time, ms

V injection velocity, $mm \cdot s^{-1}$

REFERENCES

1 Rosato, D., Plastics Processing Data Handbook, 2nd edition, Chapman & Hall, London (1997).

2 Rosato, D. V., Rosato, D. V., Injection Molding Handbook, Chapman & Hall, New York (1995).

3 Yang, Y., Adaptive control of injection molding process, M. Phil. Thesis, Hong Kong University of Science & Technology, Hong Kong (1998).

4 Zhao, Ch. H., Experimental analysis and simulation on injection molding melt temperature, M. Phil. Thesis, Hong Kong University of Science & Technology, Hong Kong (1998).

5 Wang, B. G., Gao, F., Yue, P., "Neural network prediction of melt temperature at plastication phase", Proceeding of the 2nd East Asia Polymer Conference (EAPC-2), 353—354, Hong Kong University of Science & Technology, Hong Kong (1999).

6 Taguchi, G., System of Experimental Design, White Planins, New York (1992).

7 FIDAP 8.0 *User's manual*, Fluid Dynamics International, New Jersey (1998).

8 Demuth, H., Beale M., Neural Network Toolbox-User's Guide, The Math Works Inc., (1993).